Journal of Electrocardiology 68 (2021) 56–64

Contents lists available at ScienceDirect

Journal of Electrocardiology

journal homepage: www.jecgonline.com

Pharmacological and simulated exercise cardiac stress tests produce different ischemic signatures in high-resolution experimental mapping studies

Brian Zenger [a,b,c,d,*], Wilson W. Good [a,b,c], Jake A. Bergquist [a,b,c], Lindsay C. Rupp [a,b,c], Maura Perez [a], Gregory J. Stoddard [e], Vikas Sharma [d], Rob S. MacLeod [a,b,c]

[a] Scientific Computing and Imaging Institute, University of Utah, SLC, UT, USA
[b] Nora Eccles Harrison Cardiovascular Research and Training Institute, University of Utah, SLC, UT, USA
[c] Department of Biomedical Engineering, University of Utah, SLC, UT, USA
[d] School of Medicine, University of Utah, SLC, UT, USA
[e] Department of Internal Medicine, University of Utah, SLC, UT, USA

ARTICLE INFO

Keywords:
Acute myocardial ischemia
Cardiac stress test
Experimental model
ST-segment changes

ABSTRACT

Objective: Test the hypothesis that exercise and pharmacological cardiac stressors create different electrical ischemic signatures.
Introduction: Current clinical stress tests for detecting ischemia lack sensitivity and specificity. One unexplored source of the poor detection is whether pharmacological stimulation and regulated exercise produce identical cardiac stress.
Methods: We used a porcine model of acute myocardial ischemia in which animals were instrumented with transmural plunge-needle electrodes, an epicardial sock array, and torso arrays to simultaneously measure cardiac electrical signals within the heart wall, the epicardial surface, and the torso surface, respectively. Ischemic stress via simulated exercise and pharmacological stimulation were created with rapid electrical pacing and dobutamine infusion, respectively, and mimicked clinical stress tests of five 3-minute stages. Perfusion to the myocardium was regulated by a hydraulic occluder around the left anterior descending coronary artery. Ischemia was measured as deflections to the ST-segment on ECGs and electrograms.
Results: Across eight experiments with 30 (14 simulated exercise and 16 dobutamine) ischemic interventions, the spatial correlations between exercise and pharmacological stress diverged at stage three or four during interventions ($p < 0.05$). We found more detectable ST-segment changes on the epicardial surface during simulated exercise than with dobutamine ($p < 0.05$). The intramyocardial ischemia formed during simulated exercise had larger ST40 potential gradient magnitudes ($p < 0.05$).
Conclusion: We found significant differences on the epicardium between cardiac stress types using our experimental model, which became more pronounced at the end stages of each test. A possible mechanism for these differences was the larger ST40 potential gradient magnitudes within the myocardium during exercise. The presence of microvascular dysfunction during exercise and its absence during dobutamine stress may explain these differences.

Introduction

Acute myocardial ischemia is the most common cause of chest pain and indicates many different pathologies, including Takotsubo cardiomyopathy, myocardial infarction, coronary artery disease, or coronary artery spasm [1,2]. Acute myocardial ischemia occurs in regions with inadequate perfusion, and is routinely identified noninvasively with a cardiac stress test. Cardiac stress tests monitor heart function through a 12-lead electrocardiogram (ECG) or imaging modality (*i.e.*, MRI or ultrasound) during increasing cardiovascular effort [1,3,4]. Clinically, the effort consists of a graded cardiac stressor, such as pharmacological stimulants or regulated exercise. Despite their ubiquity, the sensitivity and specificity of cardiac stress tests to acute myocardial ischemia are persistently poor, with the exercise stress tests using ECG monitoring around 55% and 65% and the dobutamine stress test using

Abbreviations and acronyms: ECG, electrocardiogram; ECGI, electrocardiographic imaging; CAD, coronary artery disease; LAD, left anterior descending coronary artery; ST40%, ST-segment 40% potential; MRI, magnetic resonance imaging; PVC, premature ventricular contraction; CEI, Consortium for Electrocardiographic Imaging.

* Corresponding author at: 72 South Campus Dr., SLC, UT 84112, USA.
E-mail address: brian.zenger@hsc.utah.edu (B. Zenger).

https://doi.org/10.1016/j.jelectrocard.2021.07.009
0022-0736/

ultrasound imaging (echocardiography) around 85% and 80%, respectively [1,3,4]. The poor detection or misdiagnosis of ischemia can lead to several adverse consequences, including accelerated cardiac decompensation or unnecessary procedural interventions.

One possible and unexplored source of this inadequate detection is differences between cardiac stress types. Cardiac stress is induced clinically using regulated exercise via treadmill walking or pharmacological stimulation via dobutamine infusion [4]. Dobutamine infusion stimulates the heart through beta-1 receptors to increase heart contractility and heart rate [5]. Regulated exercise stimulates the heart by decreasing vagal tone, increasing sympathetic stimulation, and increasing cardiac preload. Both stress methods follow explicitly defined clinical protocols. Despite the obvious mechanistic differences between pharmacological stimulation and exercise, few studies have directly compared the different stress types directly at high spatial resolution and in three dimensions. Most previous studies have compared the sensitivity and specificity of detecting ischemia using exercise with ECG and dobutamine with ultrasound echocardiography (echo)[4,6–8]. These studies report variable ranges of sensitivity and specificity, with the majority showing dobutamine with echo outperforming exercise with ECG. Some studies have examined 12-lead ECG measurements during both exercise and dobutamine stress. These studies found exercise to be significantly more sensitive and specific than dobutamine [9]. However, the authors were unable to offer a clear explanation for these differences because of the limited resolution of the 12-lead ECG. Most of these previous studies found differences in the diagnostic performance between the two cardiac stressors. However, the nature and possible mechanisms for this difference have not been well characterized in an experimental or clinical setting.

Recent advancements in large-animal experimental models of acute myocardial ischemia have made it possible to examine electrical changes during a controlled ischemic episode with high-resolution recording arrays. The biophysical basis for detecting myocardial ischemia electrically is well characterized. Remote recording electrodes measure potentials created by current flowing within the myocardium. Increased current drives increased potential measurements. In a healthy heart, no current should be flowing during the ST-segment. However, ischemic changes to cardiomyocyte action potentials create potential differences between ischemic and healthy tissue [10–12]. Under these conditions, passive current, also called injury current, flows from the relatively positive healthy tissue to the relatively negative ischemic tissue during the ST segment. [13]. Injury current appears as positive or negative deflections to the ST segment from remote recording electrodes. Injury current increases with larger potential gradients between healthy and ischemic tissue.

The goal of this study was to characterize the differences in the electrical signatures of ischemia induced via dobutamine and simulated exercise from high-resolution electrocardiographic mapping in a controlled experimental model. We chose to assess electrical changes because of their ubiquity in clinical practice and, at least at the cellular level, there is a precise biophysical mechanism for ischemic changes. Based on previous clinical studies, we hypothesized a significant difference in the ischemia developed between dobutamine and simulated exercise. We tested this hypothesis using a novel large-animal experimental preparation of acute myocardial ischemia to simulate repeated clinical cardiac stress tests under controlled conditions. We recorded the electrical signals of ischemia at high resolution (over 600 electrodes) within the heart wall (intramural), on the heart surface (epicardial), and on the torso surface. We identified ischemic signatures based on changes to the ST-segment potentials (ST40%) of electrograms (measured within the heart or on the heart surface) or electrocardiograms (measured on the torso surface).

Methods

Experimental preparation

Animal model selection and surgical procedure

The experimental preparation used in this study has been described previously in Zenger et al. [14]. Briefly, we used 30 kg male and female Yucatan minipigs because of their similar cardiovascular structure to humans and validated use in previous acute myocardial ischemia studies [14]. A midline sternotomy was performed to expose the anterior surface of the heart. The heart was suspended in a pericardial cradle, and the left anterior descending coronary artery was exposed and a hydraulic occluder was placed around the vessel. Recording arrays described below were then placed. The pericardium and chest wall were then sutured closed and checked for residual air. The animals were purpose-bred for use in experimental research. All studies were approved by the Institutional Animal Care and Use Committee at the University of Utah and conformed to the Guide for Care and Use of Laboratory Animals (protocol number 17-04016 approved on 05/17/2017).

Recording arrays

Recording arrays sampled electrical signatures within the heart wall (intramural), on the heart surface (epicardial), and on the torso surface. Each intramural plunge needle array recorded extracellular potentials at 10 depths, 1.6 mm apart. For each experiment, 20–30 needles were placed in the anterior ventricular myocardium. The epicardial sock recorded at 247 sites around both ventricles with approximately 6.6 mm^2 resolution. Finally, vertical torso strips were aligned cranial to caudal on the torso surface. Each strip had 12 electrodes, spaced 3 cm apart, and eight vertical strips were placed on the anterior torso for each experiment (Fig. 1). All signals were recorded with a custom signal acquisition system, which low-pass filtered, gain adjusted, and recorded up to 1024 channels at 1 kHz [15].

Cardiac stress test protocols

We simulated cardiac stress tests by mimicking clinical protocols. Each simulated cardiac stress test, or intervention, lasted up to 15 min, broken into five 3-min stages. Interventions were terminated if mean arterial blood pressure dropped more than 30 mmHg from baseline or a series of three or more PVCs occurred. We performed two simulated

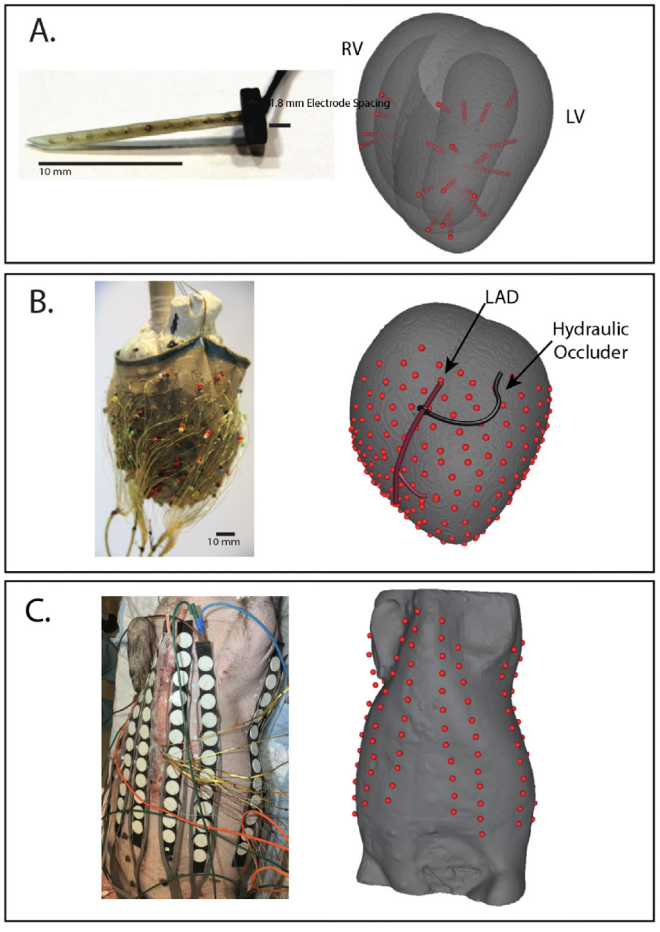

Fig. 1. Measurement domains and electrode configurations. A. Intramural plunge needle arrays in both physical form (left) and rendered (red) within the three-dimensional geometric model of the heart (right) B. Epicardial sock electrode array in both physical form (left) and registered to geometric model of the heart (right) C. Torso surface potential electrode strips in both physical form (left) and registered to the geometric model of the torso surface (right).

exercise and two dobutamine stress tests per animal. Both cardiac stressors were used in each animal to compare under identical physiological circumstances while controlling for animal-to-animal variability. The order of interventions (*i.e.*, dobutamine or simulated exercise occurring first) varied between experiments. A 30-min rest period preceded each ischemic intervention, which has been previously shown as adequate time for the heart to return to baseline [14]. Fig. 2 shows an example of signals acquired from an intramural recording electrode throughout an ischemic intervention. To reduce the effects of ischemic preconditioning, two normalization ischemia protocols were induced prior to recorded ischemic episodes. Each normalization episode lasted 10 min with occlusion and pacing.

Simulated cardiac stress

To simulate exercise stress on the heart, we paced from the right atrium at set levels above resting heart rate. The levels were based on clinical Bruce exercise stress tests shown in Table 1 and were held constant throughout each stage [16]. Pacing has been shown to produce similar ECG responses compared to exercise and is the most similar analog to exercise considering the experimental preparation [17–19]. No studies to our knowledge have performed high-resolution comparisons of pacing and exercise cardiac stress. To replicate clinical pharmacological stimulation, we used the dobutamine infusion protocols shown in Table 1. The infusion rate was held constant throughout each stage [20].

Hydraulic vessel occlusion

Perfusion deficits were created by placing a hydraulic occluder around the left anterior descending (LAD) coronary artery. The occluder controllably reduced the cross-sectional area of the LAD by 50–90%. For each experiment, the tolerated occlusion amount was determined based on cardiovascular stability (*i.e.*, maintaining sinus rhythm without trains of three or more premature ventricular contractions) and held constant throughout each ischemic intervention. Occlusion was relaxed completely during rest periods.

Signal processing

Quantification of ischemia

Signals (electrograms and electrocardiograms) were referenced to Wilson's central terminal, digitally processed, and fiducialized using the open-source PFEIFER platform [21]. Signals with unacceptable noise were manually identified and removed in the intramural case or reconstructed via Laplacian interpolation from the surrounding electrode neighborhood in the epicardial and torso surface cases. ST segment changes were used as local indicators for acute myocardial ischemia and chosen because of the regular clinical use and strong biophysical mechanism for indicating ischemia [12,22]. Specifically, for each beat, we identified the potential value at 40% of the ST segment duration (ST40%) and averaged the values over a ± 5 ms window to reduce noise or signal artifacts. The ST40% potentials for each stage were determined from recordings at the end of each stage (*i.e.*, each 3-min interval) to allow for the ischemia to reach a steady-state with consistent cardiac stress. Fig. 2 shows an example of the ST40% values on intramural electrograms as well as the sampling time points during an ischemic intervention. For torso surface recordings, we found that signals from the inferior end of each strip extended significantly into the abdomen across all animals and showed very little cardiac signal. Therefore, we removed the bottom two electrodes from each strip used in the analysis.

Geometric model generation

Following each experiment, animals were imaged postmortem in a 3-Tesla MRI scanner (Siemens Medical, Erlangen, Germany) from which the thorax as well as the needle, sock, and torso electrodes could be imaged. Following the full-thorax scan, the heart was removed, fixed, and scanned at submillimeter resolution using a 7-Tesla MRI scanner (Bruker BIOSPEC 70/30, Billerica, MA). By first segmenting (using the Seg3D software, https://www.sci.utah.edu/cibc-software/seg3d) and then merging the elements from the two MRI scans, we could construct geometric tetrahedral models using our Cleaver meshing software (https://www.sci.utah.edu/software/cleaver). Further aligning and electrode location refinement were implemented using the GRÖMER registration pipeline [23]. For intramural volumetric analyses, ST40 potentials were interpolated from intramural measurement nodes throughout the high-resolution mesh using thin-plate spline radial basis functions. Visualizations were performed using the *map3d* (https://www.sci.utah.edu/software/map3d) and SCIRun (https://www.sci.utah.edu/cibc-software/scirun) open-source software packages and MATLAB (Mathworks, MA, USA).

Table 1
Dobutamine infusion rates and heart rate increase by stage within an intervention.

Stage	Dobutamine infusion rate (μg/(kg*min))	Heart rate above resting (bpm)
1	5	37
2	10	55
3	20	76
4	30	91
5	40	102

Comparisons of ischemic electrical responses

ST40 potential values were extracted and compared at the end of each stage throughout an ischemic intervention as shown in Fig. 2. Pairwise correlation metrics were calculated between all dobutamine and pacing interventions within the same animal experiment. In a typical scenario, two simulated exercise and two dobutamine interventions were performed during an experiment. Four correlation coefficients were then calculated at each time point (dobutamine one vs. simulated exercise one, dobutamine one vs. simulated exercise two, dobutamine two vs. simulated exercise one, dobutamine two vs. simulated exercise two). Pairwise correlation values were not calculated between interventions from other experiments. We also calculated general intervention characteristic variables and compared them across interventions and experiments.

Spatial correlation of ischemic signatures

We compared ischemic signatures of simulated exercise to dobutamine stress tests using spatial correlation, which captures similarities of patterns within a recording domain (*i.e.*, intramural, epicardial, and torso surface) between two intervention types.

Clinically detectable ST40 changes on remote recording arrays

We also assessed the presence of clinically detectable ST40 changes, which we defined as ST40 potential shifts above or below set threshold values. Epicardial sock thresholds were set to potentials above 1 mV or below −0.5 mV based on the ratio between the QRS amplitude and ST-elevation thresholds used clinically. Torso-surface signal amplitude varied drastically; therefore, we thresholded the clinical signal to be two standard deviations above or below the mean ST40 potentials acquired during control recordings (no

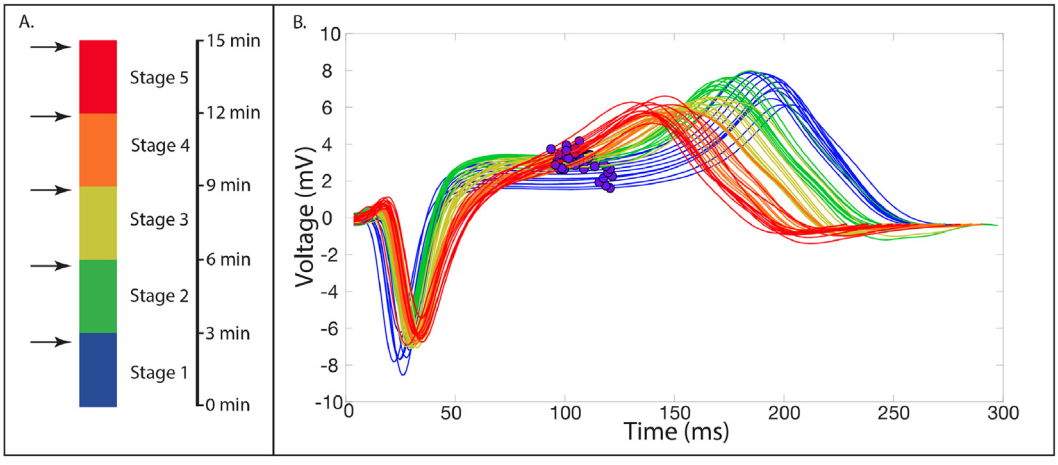

Fig. 2. Sample electrograms during a single episode of ischemia. A. The colormap applied to the electrograms, showing the stages within a single episode of ischemia with arrows indicating the ends of each stage, when we captured signals representative of the stage. B. Example electrograms from an intramural electrode during a dobutamine ischemic intervention. Purple markers indicate the ST40% potential values extracted from each of the electrograms captured at the end of the five stages.

ischemia). We then compared the number of electrodes above and below threshold in dobutamine and simulated exercise interventions.

Intramural volume analysis

Interpolated ST40 potentials within the tissue volume provided a means to identify ischemic zones, which were defined as ST40 potentials above 1 mV. We then computed the volume of these ischemic zone and compared differences in absolute ischemic-zone volume between dobutamine and simulated exercise interventions.

Ischemic zone dice overlap

Using the ischemic zones, we calculated the Dice overlap coefficient, which provides a normalized measure, between 0 and 1, of overlap between two volumes [24]. In this case, we computed the Dice overlaps between ischemic zones created from different intervention types. Excellent overlap is above 0.8, moderate above 0.6, and poor below 0.6 [24].

Intramural ST40-potential gradient magnitude analysis

Again using the interpolated ST40 potentials, we computed the gradient of electrical potential throughout the myocardial region sampled by the intramural plunge needles. To compare dobutamine and simulated exercise interventions, we averaged the top quartile of gradient magnitudes for each intervention type. We then compared differences in top quartile gradient magnitude between stress types throughout the experiments.

Statistical variability analysis of all calculated metrics

To compare intervention characteristic variables (*i.e.,* ischemic volume, gradient magnitudes, and clinical signal detection) for statistical differences, we performed a random effects multilevel regression analysis, which compensated for repeated measures within one animal experiment. We also statistically compared the correlation metrics that inherently computed differences between dobutamine and simulated exercise interventions (*i.e.,* spatial correlation and Dice overlap correlation). For correlation metrics, we determined if the computed correlation values between different intervention types were within the variability of computed correlations for identical intervention types. This analysis determines if the changes in the correlation metrics were significantly different compared to the intrinsic variability of interventions. Again, we performed a random effects multilevel regression to compensate for repeated measures within subjects. Statistical significance was defined as $p < 0.05$. The plots generated show the mean with the standard error unless otherwise noted. Statistical analysis was performed using STATA 16.1 stats software package (StatCorp, TX, USA).

Results

For this study, we used eight animals and performed 30 ischemic interventions (14 simulated exercise and 16 dobutamine). Two simulated exercise interventions were not performed because animals died from arrhythmic events prior to the final intervention. Fig. 3 shows example ST40 potentials mapped within the myocardium, on the epicardial surface, and on the torso surface during stage five (peak ischemia) of each cardiac stress type. The locations of elevated ischemic potentials were similar at multiple myocardial cross sections between dobutamine and simulated exercise interventions. The spatial correlation value comparing these intramural signals was 0.64, and the Dice overlap coefficient was 0.72. In this example figure, the positive amplitudes in the simulated exercise were markedly increased compared to dobutamine interventions (15 mV vs. 5 mV, respectively). Ischemic signatures were also larger in amplitude on the epicardial surface during simulated exercise, with higher and lower extrema than during dobutamine stress (−3.5 mV to 3.5 mV vs. −1 mV to 2 mV, respectively). The epicardial spatial correlation between these two interventions was low at 0.02. Finally, the torso-surface potentials showed marked elevations during simulated exercise that were not present during dobutamine, and the spatial correlation was 0.79.

Spatial correlation of ischemic signatures

We assessed aggregated spatial correlations to compare the two cardiac stress types based on the ST40 values from the intramural, epicardial, and torso-surface signals. As shown in Fig. 4 in red, the spatial correlation dropped substantially between different intervention types across all recording domains through all stages of the ischemic interventions. Specifically, at the end of stage one, the spatial correlation remained high (above 0.75) across all experiments. At stages two to three, the spatial correlation dropped in the intramural (0.75 to 0.6), epicardial (0.85 to 0.6), and torso surface (from 0.8 to 0.6) recordings. At the end of stage five, the mean spatial correlation was below 0.6 across all surfaces, with the epicardial surface spatial correlation at 0.2. These results show a decreased similarity of the ischemic signature patterns for different cardiac stressors across the intramural, epicardial, and torso domains as the intervention progresses (*i.e.,* from stage 1 to 5).

We also performed a statistical variability analysis to determine if the spatial correlations comparing different cardiac stress types were similar to the spatial correlations comparing identical cardiac stress types. As shown in Fig. 4, the identical comparisons had spatial correlations that remained above 0.7 throughout the interventions (blue).The spatial correlations between different intervention types were significantly lower than spatial correlations between identical intervention types. Statistical significance was identified in all stages for the needle measurements, all stages for the sock measurement, and stages one, four, and five for the torso measurements ($p < 0.05$ for all). These results show that spatial correlations between different cardiac stress types were significantly lower than spatial correlations of identical stress types throughout ischemic interventions.

Detectable signal on the epicardial and torso surfaces

We also examined a 'clinically detectable signal' on the epicardial and torso surfaces. The detectable signals used threshold cutoffs described in "Comparisons of ischemic electrical responses" section, from which we counted the numbers of electrodes that exceeded these thresholds. We observed no significant difference among the numbers of electrodes with detectable clinical signals during stages one through three on the epicardial surface (Fig. 5, $p > 0.05$). We found significantly more detectable electrodes during stages four and five during simulated exercise compared to dobutamine on the epicardium (stage 4 simulated exercise = 60 electrodes and stage 4 dobutamine = 15 electrodes $p < 0.05$, stage 5 simulated exercise = 80 electrodes and stage 5 dobutamine = 18 electrodes $p < 0.05$).

On the torso surface, no differences were found between the number of electrodes throughout the entire intervention ($p > 0.05$ for all). On average, dobutamine and simulated exercise interventions induced clinical signals in 20 to 30 torso electrodes. The number of clinically identifiable electrodes did not vary markedly between stages two through five. The standard error was large (approximately 10 electrodes) throughout stages two through five for both intervention types.

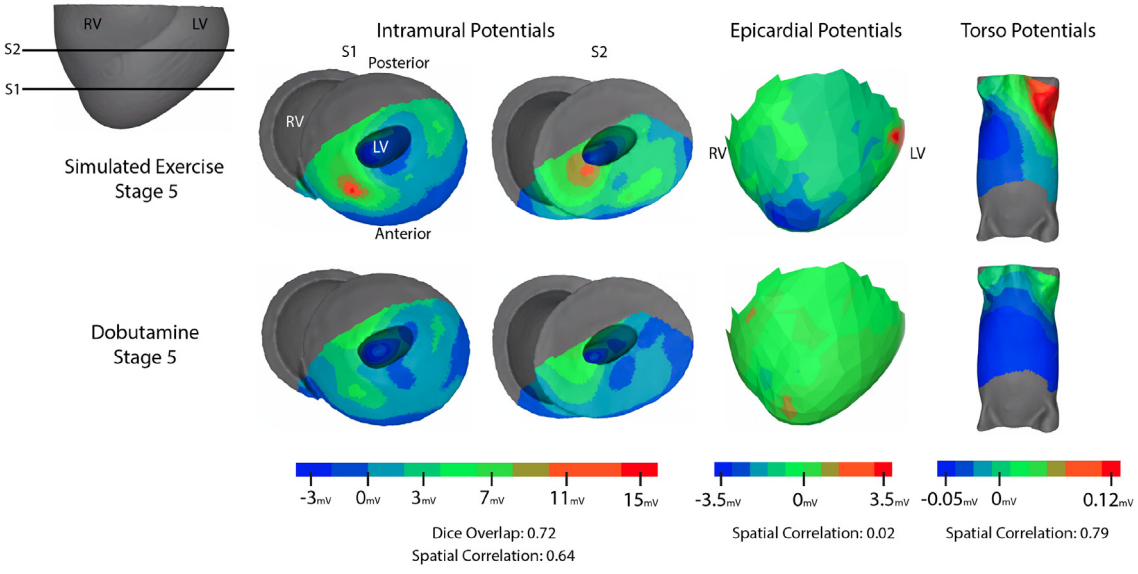

Fig. 3. Sample measured ST40 potentials. Row 1: Simulated exercise intervention stage 5. Row 2: Dobutamine intervention stage 5. Columns 1 and 2: Interpolated ST40 potentials from intromyocardial recording arrays at different basal/apical levels. Column 3: Epicardial sock potentials. Column 4: Torso surface potentials.

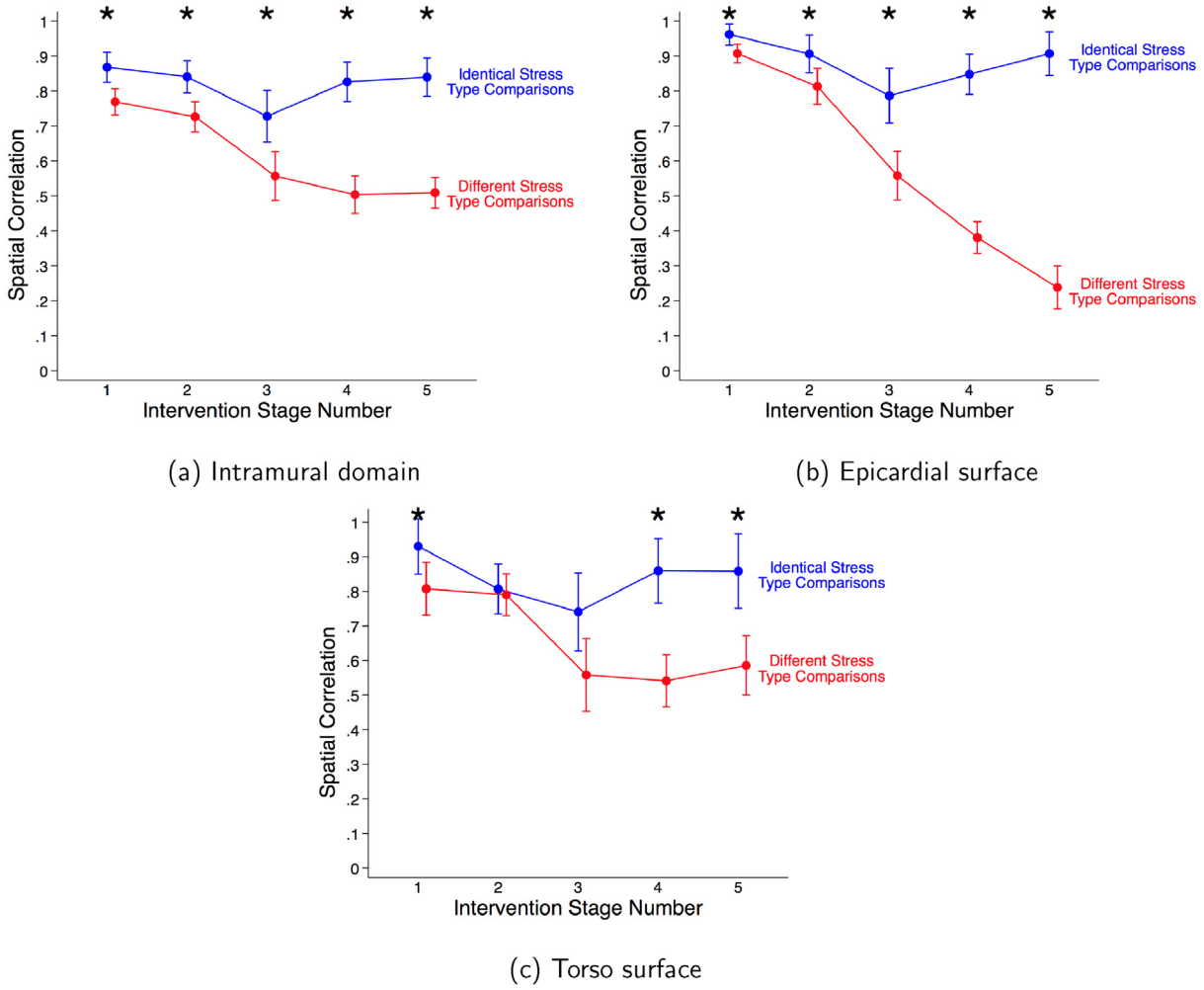

Fig. 4. Summary of spatial correlation values across all experiments comparing different cardiac stress types (dobutamine and simulated exercise). Red lines are average spatial correlation values comparing different intervention types. Blue lines are average spatial correlation values of identical intervention types. Black stars indicate statistically significant differences between identical and different spatial correlation calculations. Error bars are derived from standard error calculations.

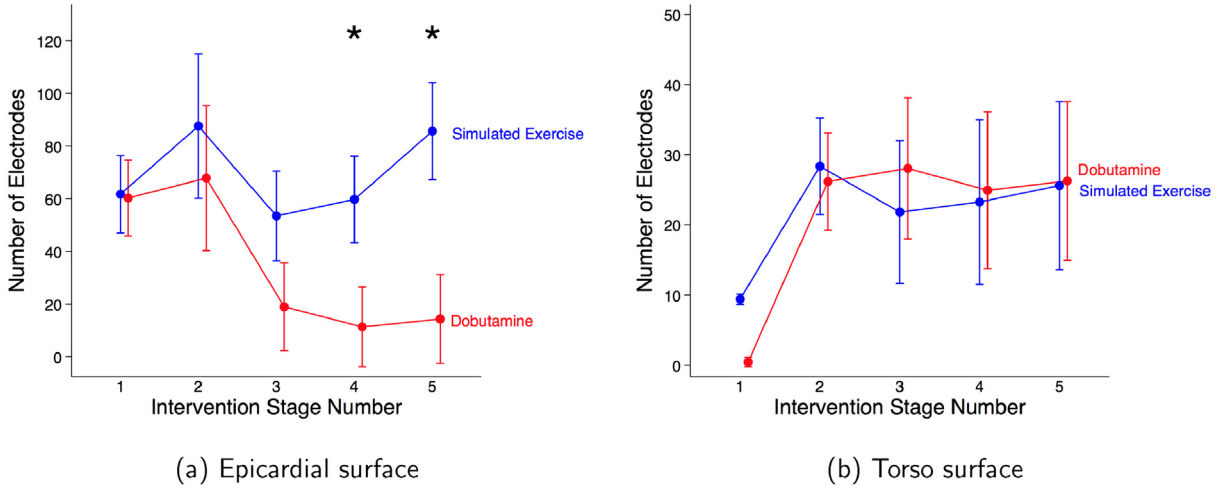

Fig. 5. Mean number of electrodes with detectable clinical signal on the epicardial (A) and torso surfaces (B). Blue lines indicate simulated exercise interventions and red lines indicate dobutamine intervention. Error bars are standard error calculations. Black stars indicate significant differences between intervention types ($p < 0.05$).

Intramural signal analysis

To determine the underlying mechanisms for the differences noted between ischemic signatures, we assessed the differences of ischemic potentials within the myocardium.

Ischemic zone volume

Using interpolated intramyocardial ST40 potentials, we assessed the changes in ischemic zone volume throughout the ischemic interventions (Fig. 6). The volume increased in stage three of the ischemic interventions (mean up to 20,000 mm^3), then for dobutamine dropped in stage 4 to amounts similar to stage one (mean 18,000 mm^3), and then rose again to slightly elevated levels (19,000 mm^3). For simulated exercise, the values rose gradually to peak at stage 4 and then returned to slightly elevated values (18,000 mm^3 vs. 16,000 mm^3). We did not identify any significant differences between the dobutamine or simulated exercise ischemic volume throughout an intervention ($p > 0.05$). From these results, we concluded there was no difference between ischemic zone volume induced via dobutamine or simulated exercise throughout the interventions.

Dice overlap

Dice overlap coefficients, which compare the spatial distribution of ischemic volumes within the myocardium (Fig. 7), showed a decreasing trend of both identical and different comparisons throughout the interventions. Specifically, Dice coefficients calculated comparing identical intervention types decreased from 0.85 and 0.75, and different comparisons decreased from 0.75 to 0.58. Statistical differences between different and identical Dice coefficient comparisons were noted at every stage throughout an intervention ($p < 0.05$ for all).

Intramural gradient magnitudes

Fig. 8 shows results of the magnitude of ischemic gradients (in mV/mm) calculated from intramyocardial ST40 values. Gradient magnitudes in both dobutamine and simulated exercise interventions varied over time (between 0.65 mV/mm and 0.93 mV/mm); however, the temporal patterns differed for the two stress types. Dobutamine gradient magnitudes initially increased to 0.85 mv/mm, but then dropped to 0.7 mV/mm, which contrasted with the results from simulated exercise. Gradients for exercise increased initially as well, but then remained constant at approx. 0.9 mV/mm for stages two through five. Simulated exercise interventions produced significantly larger gradient magnitudes than dobutamine interventions during stages four and five ($p < 0.05$).

Data availability

The explicit data used in this study are available through the figshare online repository at https://doi.org/10.6084/m9.figshare.14150057 and https://doi.org/10.6084/m9.figshare.14150069.

Discussion

The goal of this study was to test the hypothesis that significant differences exist between ischemia induced by dobutamine and simulated exercise cardiac stress. Our experimental model simulated partial blockage, demand-based ischemia with the goal of simulating clinical stress tests by matching Bruce-protocol target heart rates and dobutamine infusion rates used in humans. We identified significant differences in at least some of the electrical metrics of ischemia between dobutamine and simulated exercise interventions within the heart, on the epicardium, and on the torso surface, the three recording domains we captured. These differences became larger near the end of the interventions (stages 3–5), for example, as spatial correlations decreased and differences in the clinical signals increased, where clinical signal is defined as number of electrodes above or below ST40 threshold cutoffs. Focusing on the intramyocardial signals allowed us to explore possible mechanisms to explain the differences in ischemia generated by both stress mechanisms. We found no significant differences in the ischemic zone volumes; however, we did measure differences in the Dice overlap coefficients and ischemic potential gradient magnitudes. We propose that these two variables, spatial distribution of ischemic potentials and ischemic potential gradients, drive the differences observed on the epicardial sock and torso surface potentials.

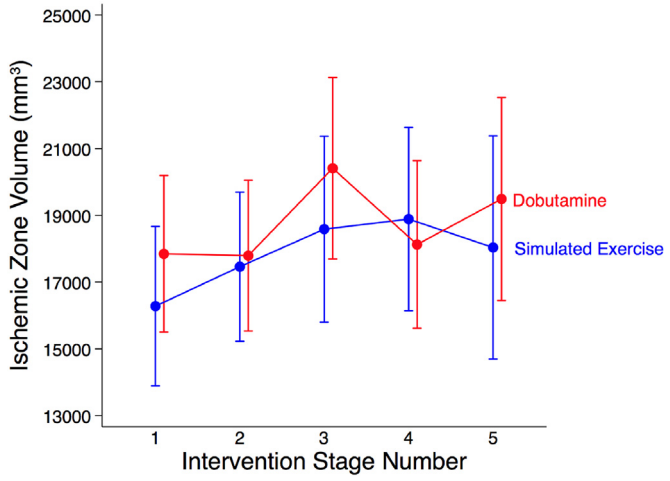

Fig. 6. Average ischemic zone volumes measured from intramyocardial electrodes throughout an ischemic intervention. Blue lines represent simulated exercise interventions, and red lines represent dobutamine interventions. No statistical significance was identified.

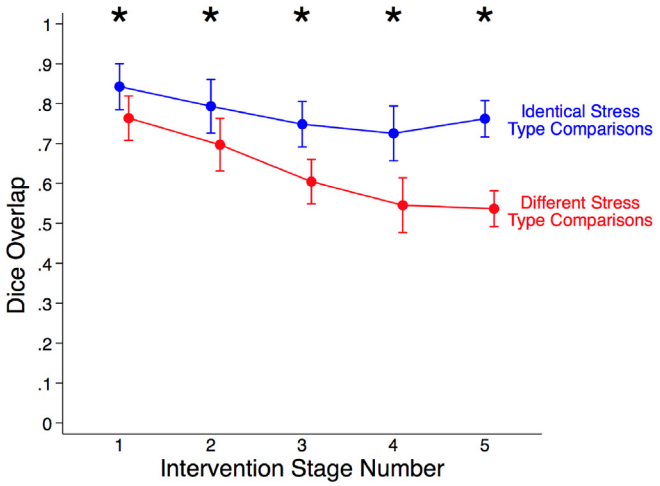

Fig. 7. Average ischemic zone volumetric Dice overlap coefficients from intramyocardial electrodes recordings. Blue lines represent dice coefficients calculated between identical intervention types, and red lines represent dice coefficients calculated between different intervention types. Black stars indicate significant differences between identical and different dice coefficient distributions ($p < 0.05$).

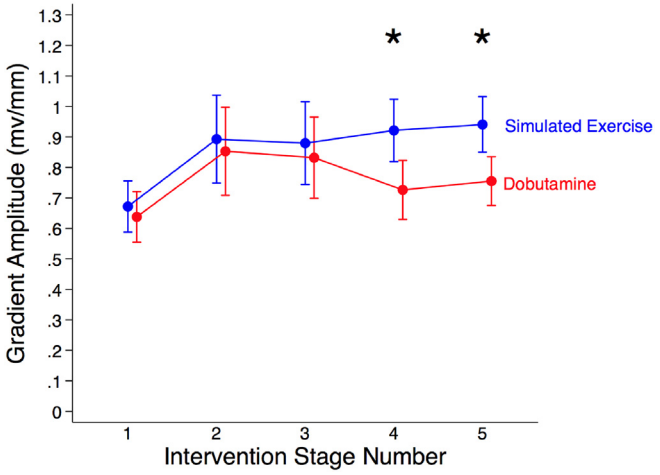

Fig. 8. Mean of the top quartile of ischemic potential gradient magnitudes throughout the recorded area of intramural plunge needles. Blue lines represent simulated exercise interventions, and red lines represent dobutamine interventions. Black stars indicate significant differences between intervention types ($p < 0.05$).

Differences in electrical signatures of ischemia between dobutamine and simulated exercise

Our findings suggest that significant differences exist between dobutamine and simulated exercise stress types, differences that appear most predominantly at the end of the ischemic interventions. Spatial correlations of ST40 potentials were significantly different throughout the interventions; however, these differences grew in the middle and later stages (3–5) (Fig. 4) across all domains. Similar patterns were visible in several other metrics, such as the ST40 shifts on the epicardium (Fig. 5), overlap of ischemic zones (Fig. 7), and gradient magnitudes of ST40 potentials (Fig. 8).

The torso surface recordings were less sensitive to these findings than cardiac signals (Fig. 5), likely for reasons shared by many ECG-based metrics. Torso signals are a spatial average of a large myocardial region and are blurred as they project to the torso surface. Epicardial potentials are much closer to the ischemic sources and capture more of their features than the torso surface, as indicated by results in Fig. 5. A further source of ambiguity is the finding that ischemic volumes were not significantly different between stressors (Fig. 6), although they had different locations, amplitudes, potential gradients, and shapes (Figs. 3, 4, 7, and 8). The ECG lacks the intrinsic resolution and sensitivity to differentiate these features. Another possible source of diminished ECG sensitivity is the experimental and natural variability between subjects. In our experiments, signal amplitude on the torso surface varied from animal to animal, likely due to difference in skin preparation and impedance as well as the closure and subsequent image-based reconstruction of the chest cavity. We applied vacuum suction to ensure minimal air remained in the chest cavity; however, a perfect seal was unlikely. Finally, the noise within the torso recordings was substantial and may have concealed electrical markers of ischemia.

Microvascular dysfunction as a possible mechanism for differences between cardiac stress types

A possible mechanistic explanation for the differences in intramural ischemic potentials is the development of microvascular dysfunction during only one of the cardiac stressors. Microvascular dysfunction is a paradoxical increase in small vessel resistance seen within ischemic tissue. During exercise or simulated exercise with pacing, clinical and experimental studies have shown the development of considerable microvascular dysfunction [25–29]. By contrast, other studies have shown that dobutamine stress decreases microvascular resistance through off-target beta-2 vasodilation [5,30]. Although our experiments lacked explicit measurements of microvascular resistance, the consistent findings in previous studies reasonably suggest microvascular dysfunction as a possible mechanism for different levels of intramyocardial perfusion and hence electrical signatures.

Our observations support the presence of microvascular dysfunction during simulated exercise because we observed more intense ischemia within underperfused regions during simulated exercise than dobutamine stress. Potential (ST40) gradients we computed within the tissue supported these findings. We found significantly larger (approximately 30%) gradient magnitudes within the myocardium during the latter stages of exercise vs. dobutamine interventions (Fig. 8). The larger gradient magnitudes indicate more severe ischemia flanked by healthy tissue even though the volume of ischemic tissue remained similar between stressors (Fig. 6). The enhanced intramyocardial potential gradient magnitudes in simulated exercise drive an increase in injury current throughout the myocardium, which increases ST40 amplitudes on remote recording electrodes. We hypothesize that dobutamine with ECG analysis performs poorly because microvascular dysfunction is diminished during dobutamine infusion, resulting in decreased ST40 amplitudes on the epicardium and torso surface. To our knowledge, this is the first reported study to suggest microvascular dysfunction as a possible mechanistic driver for differences in ECG-based detection of ischemia.

Implications for selection of clinical stress type

These results provide novel clinical insights into how to select the best stress mechanism to diagnose specific clinical pathologies. The pathology of microvascular dysfunction is becoming more recognized as a crucial component of myocardial ischemia formation and patient-reported symptoms. Patient burden is likely a complex mixture of many conditions such as CAD, coronary spasm, and myocardial infarction with nonobstructive coronary arteries (MINOCA), all of which can be linked to microvascular dysfunction [31–34]. Therefore, testing strategies to detect microvascular dysfunction have become more defined and include invasive testing, advanced imaging, and local drug challenges [33,35]. However, few studies exist that describe routine non-invasive tests for microvascular dysfunction, tests that could enhance early detection. Our findings suggest a possible means for such tests as they revealed large ischemic potential gradient magnitudes within the intramural myocardium that resulted in increases in ST40 potentials on the epicardial surface during simulated exercise stress (Figs. 8 and 5). By contrast, dobutamine stress produced smaller ischemic electrical signals, which in the clinical setting may mask patient burden by eliminating microvascular dysfunction. In pathologies with major microvascular dysfunction components, dobutamine stress testing may underdiagnose patients. Our findings suggest both a possible mechanistic basis for this insensitivity as well as an indication to rely on exercise stress when microvascular dysfunction is suspected.

Limitations

The main limitations of any study based on animals models is how well the response matches those expected in humans. We simulated exercise in anesthetized pigs through rapid pacing and simulated pre-existing coronary artery disease or vascular spasm with mechanically induced partial occlusions, which only approximate real exercise. However, this model showed similar responses to those observed during a clinical cardiac stress test and, therefore, can serve as a useful model to explore mechanisms of hyperacute ischemia [17–19]. Furthermore, each animal had both dobutamine and simulated exercise stress tests performed, which controlled for baseline differences in function. Another valuable measurement that was not recorded is blood pressure. This measurement would provide insights into the hemodynamic differences between dobutamine and simulated exercise and further clarify the differences between exercise and electrical pacing. Hydraulic occlusion may not adequately represent naturally occurring decreased perfusion to myocardial tissue, and our preparation omitted explicit measurement of the blood flow through the coronary vasculature. Additionally, we did not measure microvascular resistance changes to confirm microvascular dysfunction; however, previous experimental and clinical studies have indicted the regular presence of this dysfunction under the conditions we emulated. We also limited the measurements to electrical markers of ischemia rather than perform additional echocardiography to determine if wall motion abnormalities were present; the extreme electrical instrumentation of the heart precluded clear ultrasound imaging. We omitted baseline or control recordings in the results presented here because little ischemia was present at the beginning of either intervention type. There are drawbacks to using spatial correlation coefficients to capture differences between body surface electrical potentials, especially with the substantial signal blurring and smoothing that occurs through the torso volume. However, these metrics were still sensitive enough to reveal significant differences between responses to the two intervention types. Additionally, we could have compared intervention types across animal studies or conducted entire studies with only one intervention type. However, the goal of this study was to examine differences between intervention types within the

same individual subject. Finally, the number of animals and experiments could always be increased, although we did achieve statistical significance and measured consistent responses.

Data sharing and availability

Another contribution of this study is the geometric and electrical data collected, which will serve as material for future hypothesis testing and validation of computer simulations. The Consortium for Electrocardiographic Imaging (CEI) will manage the data from this study, making it available for analysis and collaborations. The goal of the CEI is to achieve progress in ECGI through open, international collaboration and the sharing of ideas, software, and data. The CEI uses a combination of open-source software and a data-sharing platform Experimental Data and Geometric Analysis Repository (EDGAR) to collaborate across multiple labs and disciplines, which enables substantial growth and discovery [36]. The datasets described in this study will be available on the CEI data-sharing platform, EDGAR. All software used in this study is also available with open-source licensing on the SCI Institute GitHub Page. Further, the explicit data used in this study are available through the figshare online repository at https://doi.org/10.6084/m9.figshare.14150057 and https://doi.org/10.6084/m9.figshare.14150069

The application of ECG Imaging in the measurement of ischemia is especially relevant as our findings showed clear improvements in diagnostic performance of epicardial electrograms over torso-surface ECGs. A specific goal of ECGI is to provide noninvasive access to cardiac signals by removing the blurring effects of the torso. By making available to the ECGI community geometric models and measured potentials from experiments of controlled ischemia, we will enable optimization of ECGI for this common condition that remains poorly diagnosed.

Conclusion

In conclusion, we found significant differences in the electrical signatures of ischemia induced by dobutamine and simulated exercise cardiac stressors through comprehensive measurements within the heart, on the epicardium, and on the torso surface of a porcine animal model. We have reported for the first time that exercise stress created significantly larger gradient magnitudes of ischemic potentials throughout the myocardium, which resulted in larger ST-segment potentials on the epicardium. We suggest that differences in microvascular dysfunction between the two stressor types drive these findings. The clinical implications of this study suggest dobutamine and exercise stress methods should not be considered interchangeable. Furthermore, if the suspected pathologies have substantial components of microvascular dysfunction, exercise or pacing should be used rather than dobutamine stress.

Financial support

Support for this research came from the NIH NHLBI grant no. 1F30HL149327 (Zenger); NIH NIGMS Center for Integrative Biomedical Computing (www.sci.utah.edu/cibc), NIH NIGMS grants P41GM103545 and R24GM136986 (MacLeod); the Nora Eccles Treadwell Foundation for Cardiovascular Research (MacLeod); University of Utah Population Health Research (PHR) Foundation (Stoddard); NIH NCRR and NCATS Grant no. UL1TR002538 (formerly 5UL1TR001067-05, 8UL1TR000105 and UL1RR025764) (Stoddard). No other authors have anything to disclose.

Industry relationships

Dr. Wilson W. Good has recently joined the Acutus Medical Group. None of the work written or performed for this study was affected by this relationship and there is no potential conflict.

Declaration of Competing Interest

The authors declare no conflict of interest.

Acknowledgments

We would like to acknowledge the support of the Nora Eccles Treadwell Cardiovascular Research and Training Institute staff, including Jayne Davis, Ala Booth, Wilson Lobaina, and Bruce Steadman, for preparing and maintaining equipment and coordinating experiment logistics.

References

[1] Safdar B, Ong P, Camici PG. Identifying myocardial ischemia due to coronary microvascular dysfunction in the emergency department: introducing a new paradigm in acute chest pain evaluation. Clin Ther. 2018:1–11.
[2] Bhuiya FA, Pitts SR, McCaig LF. Emergency department visits for chest pain and abdominal pain: United States, 1999–2008. NCHS Data Brief; 2010; 1–8.
[3] Stern S. State of the art in stress testing and ischaemia monitoring. Card Electrophysiol Rev. 2002;6(September):204–8.
[4] Knuuti J, Ballo H, Juarez-Orozco LE, Saraste A, Kolh P, Rutjes AWS, et al. The performance of non-invasive tests to rule-in and rule-out significant coronary artery stenosis in patients with stable angina: a meta-analysis focused on post-test disease probability. Eur Heart J. 2018;39(35):3322–30.
[5] Bartunek J, Wijns W, Heyndrickx GR, de Bruyne B. Effects of dobutamine on coronary stenosis physiology and morphology. Circulation. 1999;100(July):243–9.
[6] Shadeen J. Diagnostic value of 12-lead electrocardiogram during dobutamine echocardiographic studies. Am Heart J. 1998;136(December):1061–4.
[7] Dhond MR, Nguyen T, Whitley TB, Donnell K, Bommer WJ. Prognostic value of 12-lead electrocardiogram during dobutamine stress echocardiography. Echocardiography. 2000;17(July):429–32.
[8] Mairesse GH, Marwick TH, Vanoverschelde JLJ, Baudhuin T, Wijns W, Melin JA, et al. How accurate is dobutamine stress electrocardiography for detection of coronary artery disease?.. Comparison with two-dimensional echocardiography and technetium-99m methoxyl isobutyl isonitrile (mibi) perfusion scintigraphy. J Am Coll Cardiol. 1994;24(4):920–7.
[9] Beleslin BD, Ostojic M, Stepanovic J, Djordjevic-Dikic A, Stojkovic S, Nedeljkovic M, et al. Stress echocardiography in the detection of myocardial ischemia. Head-to-head comparison of exercise, dobutamine, and dipyridamole tests. Circulation. 1994;90(September):1168–76.
[10] Janse MJ, Kleber AG. Electrophysiological changes and ventricular arrhythmias in the early phase of regional myocardial ischemia. Circ Res. 1981;49(5):1069–81.
[11] Kléber AG, Janse MJ, Van Capelle FJ, Durrer D. Mechanism and time course of st and tq segment changes during acute regional myocardial ischemia in the pig heart determined by extracellular and intracellular recordings. Circ Res. 1978;42(5):603–13.
[12] Kornreich F, Montague T, Kavadias M, Segers J, Rautaharju P, Horacek B, et al. Qualitative and quantitative analysis of characteristic body surface potential map features in anterior and inferior myocardial infarction. Am J Cardiol. 1987;60:1230–8.
[13] Janse M, van Capelle F, Morsink H, Kleber A, Wilms-Schopman F, Cardinal R, et al. Flow of "injury" current and patterns of excitation during early ventricular arrhythmias in acute regional myocardial ischemia in isolated porcine and canine hearts. Circ Res. 1980;47(2):151–65.
[14] Zenger B, Good W, Bergquist J, Burton B, Tate J, Berkenbile L, et al. Novel experimental model for studying the spatiotemporal electrical signature of acute myocardial ischemia: a translational platform. J Physiol Meas. 2020;41(February):015002.
[15] Zenger B, Bergquist JA, Good WW, Rupp LC, MacLeod RS. High-capacity cardiac signal acquisition system for flexible, simultaneous, multidomain acquisition. 2020 Computing in Cardiology; 2020; 1–4.
[16] Okin PM, Ameisen O, Kligfield P. A modified treadmill exercise protocol for computer-assisted analysis of the ST segment/heart rate slope: methods and reproducibility. J Electrocardiol. 1986;19(October):311–8.
[17] Heller G, Aroesty J, McKay R, Parker J, Silverman K, Come P, et al. The pacing stress test: a reexamination of the relation between coronary artery disease and pacing-induced electrocardiographic changes. Am J Cardiol. 1984;54(1):50–5.
[18] Marangelli V, Iliceto S, Piccinni G, De Martino G, Sorgente L, Rizzon P. Detection of coronary artery disease by digital stress echocardiography: comparison of exercise, transesophageal atrial pacing and dipyridamole echocardiography. J Am College Cardiol. 1994;24(July):117–24.
[19] Schröder K, Völler H, Dingerkus H, Münzberg H, Dissmann R, Linderer T, et al. Comparison of the diagnostic potential of four echocardiographic stress tests shortly after acute myocardial infarction: submaximal exercise, transesophageal atrial pacing, dipyridamole, and dobutamine-atropine. Am J Cardiol. 1996;77(11):909–14.
[20] Mannering D, Cripps T, Leech G, Mehta N, Valantine H, Gilmour S, et al. The dobutamine stress test as an alternative to exercise testing after acute myocardial infarction. Br Heart J. 1988;59(May):521–6.
[21] Rodenhauser A, Good W, Zenger B, Tate J, Aras K, Burton B, et al. PFEIFER: preprocessing framework for electrograms intermittently fiducialized from experimental recordings. J Open Source Softw. 2018;3(21):472.
[22] Aras K, Burton B, Swenson D, MacLeod R. Sensitivity of epicardial electrical markers to acute ischemia detection. J Electrocardiol. 2014;47(6):836–41.

[23] Bergquist JA, Good WW, Zenger B, Tate JD, MacLeod RS. GRÖMeR: a pipeline for geodesic refinement of mesh registration. Lecture notes in computer science, vol. 11504. Functional Imaging and Model of the Heart (FIMH), Springer Verlag; 2019; 37–45.
[24] Dice LR. Measures of the amount of ecologic association between species. Ecology. 1945;26(3):297–302.
[25] Duncker D. Regulation of coronary vasomotor tone under normal conditions and during acute myocardial hypoperfusion. Pharmacol Ther. 2000;86(April):87–110.
[26] Chamuleau SAJ, Siebes M, Meuwissen M, Koch KT, Spaan JAE, Piek JJ. Association between coronary lesion severity and distal microvascular resistance in patients with coronary artery disease. Am J Physiol-Heart Circ Physiol. 2003;285(November):H2194–200.
[27] Gianmario S, Mario M, Paolo M, Jan S-E, Enri G, Oberdan P, et al. Coronary vasoconstriction during myocardial ischemia induced by rises in metabolic demand in patients with coronary artery disease. Circulation. 1997;95(June):2652–9.
[28] Duncker DJ, Bache RJ. Regulation of coronary blood flow during exercise. Physiol Rev. 2008;88(July):1009–86.
[29] Sambuceti G, Marzilli M, Fedele S, Marini C, L'Abbate A. Paradoxical increase in microvascular resistance during tachycardia downstream from a severe stenosis in patients with coronary artery disease: reversal by angioplasty. Circulation. 2001;103(19):2352–60.
[30] Bartunek J, Wijns W, Heyndrickx GR, de Bruyne B. Effects of dobutamine on coronary stenosis physiology and morphology. Circulation. 1999;100(July):243–9.
[31] Pasupathy S, Tavella R, Beltrame JF. Myocardial infarction with nonobstructive coronary arteries (MINOCA). Circulation. 2017;135(April):1490–3.
[32] Ong P, Athanasiadis A, Hill S, Schäufele T, Mahrholdt H, Sechtem U. Coronary microvascular dysfunction assessed by intracoronary acetylcholine provocation testing is a frequent cause of ischemia and angina in patients with exercise-induced electrocardiographic changes and unobstructed coronary arteries. Clin Cardiol. 2014;37(August):462–7.
[33] Lanza GA, Crea F. Primary coronary microvascular dysfunction. Circulation. 2010;121(June):2317–25.
[34] Kaski JC, Crea F, Gersh BJ, Camici PG. Reappraisal of ischemic heart disease: fundamental role of coronary microvascular dysfunction in the pathogenesis of angina pectoris. Circulation. 2018;138(14):1463–80.
[35] Ong P, Safdar B, Seitz A, Hubert A, Beltrame JF, Prescott E. Diagnosis of coronary microvascular dysfunction in the clinic. Cardiovasc Res. 2020;116(March):841–55.
[36] Aras K, Good W, Tate J, Burton B, Brooks D, Coll-Font J, et al. Experimental data and geometric analysis repository: EDGAR. J Electrocardiol. 2015;48(6):975–81.